Differential RNA-Dependent ATPase Activities of Four rRNA Processing Yeast DEAD-Box Proteins[†]

Ivelitza Garcia and Olke C. Uhlenbeck*

Department of Biochemistry, Molecular Biology, and Cellular Biology, Northwestern University, 2205 Tech Drive, Hogan 2-100, Evanston, Illinois 60208

Received August 26, 2008; Revised Manuscript Received October 1, 2008

ABSTRACT: *S. cerevisiae* ribosome biogenesis is a highly ordered and dynamic process that involves over 100 accessory proteins, including 18 DExD/H-box proteins that act at discrete steps in the pathway. Although often termed RNA helicases, the biochemical functions of individual DExD/H-box proteins appear to vary considerably. Four DExD/H-box proteins, Dbp3p, Dbp4p, Rok1p, and Rrp3p, involved in yeast ribosome assembly were expressed in *E. coli*, and all were found to be active RNA-dependent ATPases with k_{cat} values ranging from 13 to 170 min^{-1} and K_M(ATP) values ranging from 0.24 to 2.3 mM. All four proteins are activated by single-stranded oligonucleotides, but they require different chain lengths for maximal ATPase activity, ranging from 10 to >40 residues. None of the four proteins shows significant specificity for yeast rRNA, compared to nonspecific control RNAs since these large RNAs contain multiple binding sites that appear to be catalytically similar. This systematic comparison of four members of the DExD/H-box family demonstrates a range of biochemical properties and lays the foundation for relating the activities of proteins to their biological functions.

DEAD-box proteins are essential participants in all aspects of RNA metabolism including pre-mRNA splicing, ribosome biogenesis, RNA interference, translation, mRNA transport, localization, and decay (*1, 2*). As part of the superfamily 2 group of helicases, these proteins are classically defined by a core of nine conserved motifs important for their functional roles in RNA metabolism (*3, 4*). Structural studies have demonstrated that DEAD-box proteins fold into two covalently linked RecA-like domains in which the nine conserved motifs form an ATP-binding pocket as well as an RNA-binding site (*5*−*8*). Additionally, most DEAD-box proteins contain flanking N- and/or C- terminal extensions (NTEs or CTEs[1]) proposed to be involved in RNA binding or in the recruitment of other factors (*9*−*12*). Members of the DEAD-box family are extremely versatile given that their proposed functions include modulation of RNA−RNA, protein−RNA, and/or protein−protein interactions (*11*−*13*). These motor proteins undergo a cycle of RNA and ATP binding, ATP hydrolysis, and conformational changes that, in some cases, results in RNA helicase activity *in vitro* (*1, 14*−*18*). Regardless of the capability of DEAD-box proteins to unwind RNA, their function is coupled to their ability to bind and hydrolyze ATP (*12, 19*−*27*).

Eukaryotic ribosome biogenesis occurs primarily within the nucleolus and involves over 100 *trans*-acting factors that participate in a complex assembly pathway involving the sequential cleavage of the 35S pre-rRNA transcript, the post-transcriptional modification of approximately 110 residues, and the binding of 80 ribosomal proteins (*28*−*30*). Genetic and precursor probing experiments established that 14 out of 25 *S. cerevisiae* DEAD-box proteins contribute to rRNA processing at discrete steps within the rRNA biogenesis pathway (Figure 1A) (*2, 31*). Twelve of the 14 *S. cerevisiae* DEAD-box proteins are essential for ribosome maturation. Additionally, pull-down and yeast-two hybrid studies have confirmed the association of several DEAD-box proteins with precursor rRNAs (*32*). Point mutations in the ATPase active site indicate that ATP hydrolysis is required for proper rRNA processing (*20, 21*).

The four yeast DEAD-box proteins, Dbp3p, Dbp4p, Rok1p, and Rrp3p, chosen for this study have varied proposed functions in ribosome biogenesis (Figure 1A). Although Dbp3p is not essential for growth, its genetic depletion yields delayed cleavage of the first internal spacer (ITS1) at the A3 site (*33*), which is mediated by the endonuclease RNase MRP (*28, 34*−*37*). Dbp4p was originally identified as a multicopy suppressor of a mutation in the snoRNA U14 (*38*), which is a C/D-box snoRNA critical for the 2′-O-methylation of the 18S rRNA at position 414 as well as for cleavage at the A0-A2 sites (*39*−*41*). Depletion of Dbp4p yields a dramatic accumulation of the snoRNA U14 bound to the pre-rRNA, suggesting that Dbp4p is required for U14 release (*42*). Depletion of Rok1p also

[†] This work was funded by National Institutes of Health Grant R01-GM60268-08 (to O.C.U.) and by a postdoctoral fellowship from The American Cancer Society (to I.G.).

* Corresponding author. Tel: (847) 491-5139. Fax: (847) 491-5444. E-mail: o-uhlenbeck@northwestern.edu.

[1] Abbreviations: NTEs or CTEs, N- and/or C- terminal extensions; ITS1, first internal spacer (ITS1) of the yeast pre-rRNA; T7, T7 RNA polymerase; SDS, sodium dodecyl sulfate; LB, Luria broth; IPTG, isopropyl β-D-1-thiogalactopyranoside; Ni-NTA, nickel-nitrilotriacetic acid; Hepes, 4-(2-hydroxyethyl)-1-piperazineethanesulfonic acid; EDTA, ethylenediaminetetraacetic acid; Tris, tris(hydroxymethyl)aminomethane; DTT, DL-dithiothreitol; Mes, 2-(*N*-morpholino)ethanesulfonic acid; PK-LDH, pyruvate kinase-lactate dehydrogenase; Mops, 3-(*N*-morpholino)-propanesulfonic acid; mer, oligomer; nt, nucleotide; PCR, polymerase chain reaction; TLC, thin-layer chromatography; snoRNA, small nucleolar RNA; snoRNP, small nucleolar ribonucleoprotein.

10.1021/bi8016119 CCC: $40.75 © 2008 American Chemical Society
Published on Web 11/01/2008

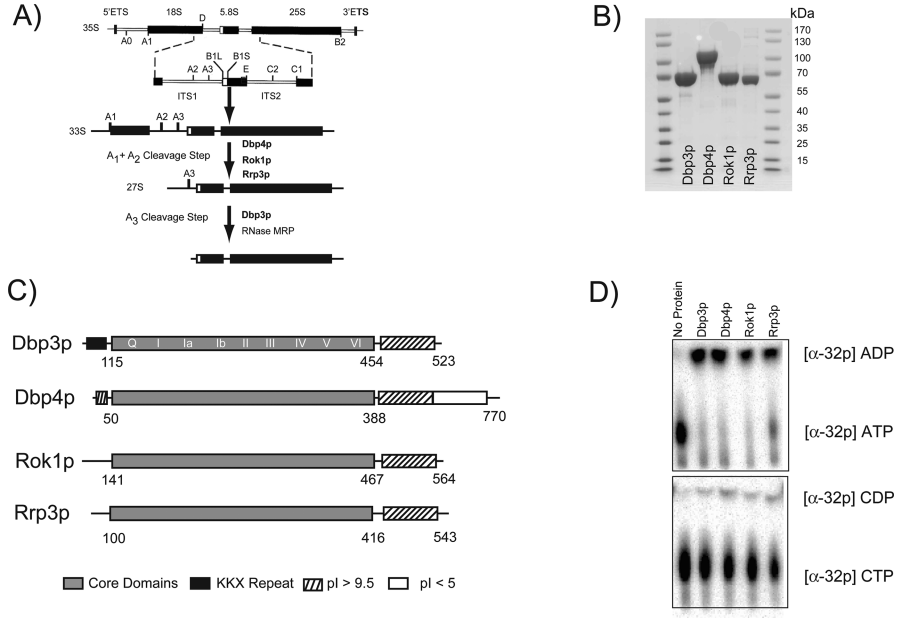

FIGURE 1: Characteristics of four yeast DEAD-box proteins. (A) Yeast pre-rRNA cleavage pathway with the main processing steps facilitated by Dbp3p, Dbp4p, Rok1p, and Rrp3p (highlighted in bold). (B) Purified proteins analyzed on a 4−15% SDS−polyacrylamide gel. (C) Structural organization of the four proteins. Residues numbered below each protein indicate the boundaries of the conserved helicase core domain. (D) Analysis of the nucleotide specificity of each recombinant protein in the presence of yeast rRNA utilizing PEI cellulose thin-layer chromatography. Reactions were performed at 30 °C in 50 mM Hepes, pH 7.5, 25 mM KCl, 5 mM MgCl2, 1 mM DTT, and 5 mM NTP-Mg^{2+}, and trace [α^{-32}P] NTP.

hinders cleavage of the pre-rRNA at sites A0, A1, and A2 (*43*). Rok1p exhibits a synthetic lethal interaction (*27, 43*) with the H/ACA-box snoRNA snR10 critical for the pseudouridylation of the 25S rRNA at position 2923 (Figure 1A) (*28, 44−46*). Finally, Rrp3p is required for fidelity of early pre-RNA cleavage (Figure 1A) (*47*). Genetic depletion resulted in reduced cleavage at the A0-A2 sites and in an aberrant cleavage between sites A2 and B1L (*47*). A more precise definition of facilitated RNA or RNP rearrangements catalyzed by each DEAD-box protein will require the isolation and structural characterization of the appropriate processing intermediates that accumulate *in vivo*. This is a daunting task because of the size of the RNP particles, which contain more than numerous ribosomal proteins and *trans*-acting factors.

An alternative approach to understanding the individual functions of the DEAD-box proteins involved in rRNA processing is to study their biochemical activities as purified proteins in the presence of rRNA substrates as well as other nonspecific RNA substrates (*26, 47−49*). While such an approach has the obvious disadvantage of not studying the function of the protein with physiological RNP substrates, it permits the establishment of the catalytic capabilities of each enzyme. As seen with other helicases, clues to RNA substrate specificity can be obtained with such purified systems (*48, 50*). These experiments lay the foundation for future *in vitro* work with more physiologically relevant substrates. Examples of the value of developing purified systems include studies with the DNA repair UvrABC helicase (*51*) and the chromosome remodeling SWI1/SNF2 helicase (*52, 53*). Hence, the selected four DEAD-box proteins, Dbp3p, Dbp4p, Rok1p, and Rrp3p, that were involved in ribosome processing were analyzed biochemically, under similar conditions and with similar substrates, to begin to understand the varied catalytic requirements of each protein. Unlike several other yeast rRNA DEAD-box proteins, Dbp3p, Dbp4p, Rok1p, and Rrp3p were soluble and active when expressed in bacteria. Therefore, this article characterizes the RNA-dependent ATPase activity for each protein and explores its individual substrate specificity.

MATERIALS AND METHODS

Cloning, Expression, and Purification of Dbp3p, Dbp4p, Rok1p, and Rrp3p. The genes for DBP3, DBP4, ROK1, and RRP3 were amplified from the *S. cerevisiae* strain Lhy1 (*54*) by hot-start PCR with Pfu DNA polymerase. The selected PCR primers introduced an N-terminal His_6 encoded sequence for affinity purification and unique restriction enzyme sites for cloning into the pET-17b expression vector. DNA sequencing utilizing the T7 promoter and terminator primers, as well as internal primers, verified each expression plasmid.

Plasmids were freshly transformed into *E. coli* BL21-CodonPlus(DE3)-RIL cells (Stratagene) and plated on carbenicillin (50 μg/mL) and chloramphenicol (50 μg/mL) LB plates. An individual colony was used to inoculate a starter culture (100 mL LB-broth) that was grown at 37 °C to an OD_{600} of 0.3. Starter cultures were spun down and resuspended in 5 mL of fresh LB-broth. The resuspended starter culture was added to 1500 mL of LB-broth containing chloramphenicol and carbenicillin and grown at 37 °C to an OD_{600} of 0.3. Cells were subsequently cooled on ice, induced with 0.8 mM IPTG for 12 h at 18 °C, and harvested by centrifugation. Cell pellets were resuspended in 30 mL of buffer A (50 mM Hepes, pH 7.5, 1 M NaCl, 10 mM $MgCl_2$, 0.1% TritonX, 5 mM β-mercaptoethanol, and 10% glycerol) containing one complete protease inhibitor cocktail tablet (Roche) and passed through a French Press twice at 8000 psi for cell disruption. The crude lysate was cleared of insoluble materials by centrifugation at 15,500 relative centrifugal force (RCF) for 15 min in a 50 mL Falcon tube with an Eppendorf 5804R. Subsequently, the supernatant was

centrifuged for an additional hour at 186,000 RCF with a Ti-45 rotor in a Beckman Optima LE-80K ultracentrifuge. Each supernatant was mixed with 5 mL of Ni-NTA (Qiagen) equilibrated with 5 mM imidazole buffer (buffer A and 5 mM imidazole), and proteins were allowed to bind the resin for 1 h at 4 °C. The bound Ni-NTA slurry was packed into a gravity column, and the column was washed with 15 mL of imidazole buffer containing one complete protease inhibitor cocktail tablet (Roche). The column was subsequently washed with 15 mL of buffer B (50 mM Hepes, pH 7.5, 500 mM NaCl, 5 mM β-mercaptoethanol, 10% glycerol, 10 mM $MgCl_2$, and 10 mM imidazole). Proteins were eluted off the column with 20 mL of 50 mM Hepes, pH 7.5, 500 mM NaCl, 5 mM β- mercaptoethanol, 10% glycerol, and 200 mM imidazole. Eluted proteins were subsequently diluted with 50 mM Hepes, pH 7.5, 5 mM β- mercaptoethanol, and 10% glycerol to obtain a final NaCl concentration of 350 mM and passed through a Mono Q column (Pharmacia Mono Q HR 5/5; 1 mL) equilibrated with 50 mM Hepes, pH 7.5, 350 mM NaCl, 5 mM β- mercaptoethanol, and 10% glycerol to remove nucleic acids. The proteins did not bind to the column and were recovered in the flow through. To prevent protein precipitation, the sodium chloride concentration in each flow through was quickly increased to 500 mM. Subsequently, each protein was concentrated with an Amicon Ultra concentrator to a final volume of 5 mL. Each protein was further purified with a gel-filtration column (Pharmacia Hiload 16/60 Superdex 200; 120 mL) equilibrated with 50 mM Hepes, pH 7.5, 500 mM NaCl, 5 mM β- mercaptoethanol, and 10% glycerol. The predominant protein peak was fractionated and activity verified by monitoring ATP hydrolysis. Proteins were dialyzed against 50 mM Hepes, pH 7.5, 500 mM NaCl, 2 mM DTT, 0.1 mM EDTA, and 55% glycerol and stored at −80 °C. Proteins remained active for up to two years of storage. A typical yield was approximately 13 mg protein/L of culture for Dbp3p and approximately 5 mg protein/L of culture for Dbp4p, Rok1p, and Rrp3p.

RNA Substrate. RNA and DNA homopolymers, poly (I:C), poly (dA-dT), and DNA substrates were purchased from Sigma Aldrich. A nested set of 11 single-stranded oligonucleotides was purchased from Dharmacon. The longest oligonucleotide was a 42-mer with the sequence: GCGAUA-AU-AA-UA-AAU-ACA-ACA-CCAUA-CACAAA-CCAAA-CCAAA. Shorter oligomers were versions of the 42-mer truncated on the 3′ end at the dashes creating 10 oligomers ranging from 6 to 37 nucleotides long. *E. coli* rRNAs (16S and 23S) were isolated from midlog *E. coli* MRE 600 cells, and *S. cerevisiae* rRNAs (18S and 25S) were isolated from midlog *S. cerevisiae* EJ101 cells utilizing an improved SDS-Urea extraction method (*19*). Harvested cells were resuspended in rRNA Lysis Buffer (50 mM Tris-HCl, pH 7.5, 10 mM $MgCl_2$, 100 mM NH_4Cl, 0.5 mM EDTA, and 6 mM DTT) with RQ1 DNase (Promega) at a ratio of 20 mL of Lysis Buffer/1.5 L of culture. Cells were lysed with a French Press and ribosomes collected via ultracentrifugation for an hour at 186,000 RCF in a Ti-45 rotor. Ribosome pellets were resuspended in 10 mM Tris at pH 7.8, 10 mM EDTA, 350 mM NaCl, 6 M Urea, and 0.1% SDS and incubated at 65 °C for 10 min. Ribosomal proteins were removed by six sequential phenol/chloroform extractions (1:1). rRNAs were ethanol precipitated, LiCl precipitated, and further purified with NAP-25 (Amersham Biosciences) columns. Subsequently, rRNAs were concentrated with ethanol precipitation (yield = 3−5 mg rRNA/L of culture).

Several RNA substrates were prepared by runoff transcription with T7 RNA polymerase. Transcription reactions were carried out in 80 mM Tris at pH 7.5, 20 mM DTT, 2 mM Spermidine, 0.1% triton, 12 mM $MgCl_2$, 0.004 U/mL pyrophosphatase, 4 mM NTP, and 0.1 mg/mL T7 RNA polymerase at 37 °C for 4 h. Yeast 35S pre-rRNA was transcribed from the plasmid pD linearized (*55*) with *Pst*I. *Tetrahymena* Group I Intron L-21 was transcribed from the plasmid pTL-21 linearized with *Sca*I (*56*). Blue Script RNA was transcribed by linearizing the pBluescript II KS (Stratagene) with *Ava*I*I* to produce a 1545 nt Blue RNA. The RNase MRP RNA, U14 snoRNA, and snR10 snoRNA were transcribed from PCR products that contained T7 promoters and blunt ends that formed runoff templates. RNAs were purified by phenol/chloroform extraction, NAP-25 size exclusion, and ethanol precipitation as described above. RNAs were stored at −20 °C in 10 mM Tris-HCl at pH 7.5. Prior to use, RNAs were heated to 95 °C for 30 s and cooled slowly to room temperature.

ATPase Assay. The rate of ATP hydrolysis was measured using the previously described coupled spectroscopic assay on microtiter plates at room temperature (*9*). For determining k_{cat} and K_M(ATP), hydrolysis rate curves were obtained at 25 °C in 50 mM Hepes, pH 7.5 (50 mM Mes, pH 6.5 for Rok1p), 25 mM KCl, 5 mM $MgCl_2$, 1 mM DTT, 200 μM NADH, 1 mM phospho(enol)pyruvate, 13−26 μg/mL lactate dehydrogenase, and 23 μg/mL pyruvate kinase at 500 nM rRNA and ATP concentrations ranging from 0.39 to 8 mM. For determination of k_{max} and K_{app}(RNA), hydrolysis curves were obtained with the same buffer at 6 mM ATP-Mg^{2+} and 12 RNA concentrations that span from 0.1 K_{app}(RNA) to approximately 4 K_{app}(RNA). The hydrolysis curves consistently resulted in single exponentials and were fit to a Michaelis−Menten equation. All values are the average of at least three independent data sets and are reported with the indicated standard deviation.

ATPase activity was also monitored by the conversion of [α-^{32}P] NTP to [α-^{32}P] NDP. Reactions contained 50 mM Hepes, pH 7.5, 25 mM KCl, 5 mM $MgCl_2$, 1 mM DTT, and 5 μM NTP-Mg^{2+}, and trace [α-^{32}P] NTP, and were incubated at 30 °C for 2 h and quenched with EDTA to 25 mM. Reaction products were separated on PEI-cellulose thin layer plates developed with 1 M LiCl and 0.5 M formic acid.

RESULTS

Cloning and Purification of Dbp3p, Dbp4p, Rok1p, and Rrp3p. E. coli expression plasmids were constructed for Dbp3p, Dbp4p, Rok1p, and Rrp3p with an N-terminal His_6-tag and transformed into a host strain that supplies additional copies of the rare arginine, isoleucine, and leucine tRNA genes (BL21-CodonPlus-RIL). To enhance protein solubility, cultures were induced with low levels of IPTG at 18 °C. Each protein was purified from cell lysates by nickel affinity chromatography and further purified by mono Q and size exclusion chromatography to eliminate nucleic acid and ribonuclease contamination. During size exclusion, all four purified proteins migrated as monomers. As determined by SDS−polyacrylamide gel electrophoresis, each protein was

greater than 95% pure (Figure 1B). Even though the purification procedure was identical for Dbp3p, Dbp4p, Rok1p, and Rrp3p, each protein has unique characteristics. In addition to the nine classically defined motifs that define the DEAD-box subgroup (Figure 1C), each protein contains positively charged (pI > 9.5) N- and/or C- terminal extensions (NTE and CTE) that have the potential to bind RNA and are likely important for each individual function (*42*). For example, Dbp3p has both a positive patch of amino acids and a lysine repeat motif within the NTE (Figure 1C) (*33*), while the CTE of Dbp4p contains both distinct basic and acidic regions (Figure 1C). As a result, all four proteins are basic with a calculated pI of 9.15 for Dbp3p, 9.86 for Rok1p, and 9.23 for Rrp3p. Because of the presence of an acidic region, Dbp4p is least basic with a pI of 7.44.

Initial Characterization of RNA-Dependent ATPase Activity. The DEAD-box protein family contains a unique conserved Q motif that was identified as an adenine recognition motif necessary for selective hydrolysis of ATP or dATP (*4*). However, certain DEAD-box proteins can bind GTP, CTP, and UTP with relatively similar binding affinities and stimulate duplex unwinding in the absence of hydrolysis (*58*). Therefore, the nucleotide specificity of Dbp3p, Dbp4p, Rok1p, and Rrp3p was directly measured by monitoring the hydrolysis of subsaturating [α-^{32}P] NTP or [α-^{32}P] dATP in the presence of 500 nM yeast rRNA by thin-layer chromatography (Figure 1D). Similar to previously characterized DEAD-box proteins (*14, 26, 50*), Dbp3p, Dbp4p, Rok1p, and Rrp3p hydrolyzed dATP and ATP to completion, while GTP, UTP, and CTP showed negligible hydrolysis after 2 h (Figure 1D). For all four proteins, high concentrations (6 mM) of GTP, UTP, or CTP appreciably inhibited the ATPase activity suggesting that each protein can bind all NTPs (data not shown). Nevertheless, the NTP hydrolysis event that is required for proper rRNA processing *in vivo* only occurs in the presence of ATP hydrolysis (*20, 21*).

A spectrophotometric ATP hydrolysis assay was utilized to establish the effect of pH and ionic strength on the rate of hydrolysis for each DEAD-box protein. Since utilizing the appropriate ribosomal assembly intermediate as a substrate is currently not possible, assays were primarily performed with fully mature yeast rRNA, although similar results were obtained with an unmodified pre-rRNA (35S) transcript. Experiments were performed at saturating 6 mM ATP-Mg^{2+} and at 500 nM rRNA, which were both in molar excess over the protein to ensure that no competition occurs for a favored site. The pH dependence of ATP hydrolysis was measured for each protein between pH 5.5 and 9.5 utilizing three buffers that were compatible with the PK-LDH coupling enzymes of the spectroscopic assay. As shown in Figure 2, the pH-rate profiles of the four proteins were quite similar. Each protein demonstrates a broad optimum between pH 7 and 9, with a decrease in activity at or below pH 6. This behavior is similar to the *E. coli* ribosomal DEAD-box protein DbpA (*48*). However, other members of this protein family displayed a true pH optimum for ATP hydrolysis (*26, 57*). In the absence of RNA, the ATPase activities of Dbp3p, Dbp4p, and Rrp3p were greatly diminished, compared to the activity observed in the presence of RNA, and showed negligible pH dependences (open symbols, Figure 2). Dbp3p and Rrp3p were stimulated 10-fold upon the addition of RNA, while Dbp4p was stimulated 60-fold (Table 1).

Unlike the other three proteins, Rok1p showed an RNA-independent rate of ATP hydrolysis in both Hepes and Mops buffers that approach the rate observed in the presence of RNA (closed vs open symbols, Figure 2). This RNA-independent activity was unlikely due to RNA contamination in the enzyme preparation since preincubation of Rok1p with 0.025 mg/mL of RNase A for 15 min does not affect this activity (data not shown). In addition, the observed RNA-independent activity in Hepes at pH 7 was noted previously and shown to be sensitive to mutations within motif I, which indicates that the activity is not due to a contaminating ATPase (*27*). Surprisingly, Rok1p showed a much lower RNA-independent ATPase activity when assayed in Mes buffer between pH 5.5 and pH 6.9 (Figure 2). Under these conditions, Rok1p was stimulated 10-fold with the addition of RNA, similar to Dbp3p, Dbp4p, and Rrp3p (Table 1). It is unlikely that the lower RNA-independent activity is due to the lower pH of the Mes buffer. At pH 6.5 and pH 6.9, both Mops and Mes buffers possessed similar RNA-dependent rates of ATP hydrolysis, yet the RNA-independent rate was observed to be dramatically less in the Mes buffer (Figure 2). At this time, it is not fully understood why Rok1p had such interesting buffer specific activities. These results clearly show the merit of extensive examination of the reaction components when analyzing a new enzyme. Subsequent experiments exploring the RNA-dependent ATPase activity of Rok1p were performed in Mes, pH 6.5.

The ATPase activity of all four proteins was also measured at varying $MgCl_2$ and KCl concentrations in the presence of saturating ATP and RNA with either Mes or Hepes buffers. As the Mg^{2+} concentration was increased from 0 to 5 mM, the reaction rate increased, which is consistent with the chelation of magnesium by the 6 mM ATP (data not shown). Further increasing the Mg^{2+} from 5 mM to 12 mM did not have an effect on the observed rate of ATP hydrolysis. In contrast, when the KCl concentration was increased from 20 mM to 150 mM, the observed hydrolysis rate for all four proteins decreased at varying slopes (Figure 3). In the case of Rok1p and Rrp3p, an ionic strength greater than 110 mM resulted in nearly immeasurable hydrolysis rates with the spectroscopic coupled assay. The slopes of the KCl dependence for Dbp4p, Rok1p, and Rrp3p were within 2-fold (-0.16 to -0.071 $min^{-1}mM^{-1}$; Figure 3). Dbp3p demonstrated a much greater dependency on KCl concentration (slope of -1.1 $min^{-1}mM^{-1}$) when compared to Dbp4p, Rok1p, and Rrp3. In all four cases, the observed decrease in ATP hydrolysis activity at higher ionic strengths was not the result of weaker RNA or ATP binding because control experiments showed that both concentrations remained saturating even in the presence of the highest salt concentration. Presumably, the organization of the ATP binding pockets in all four proteins is affected by the concentration of KCl, which may compete with one or more interactions that are important for catalysis but not for RNA and ATP binding.

Kinetic Characterization of ATP Hydrolysis. The rate of ATP hydrolysis for Dbp3p, Dbp4p, Rok1p, and Rrp3p was measured as a function of ATP concentration at saturating rRNA (500 nM) and analyzed by Michaelis−Menten kinet-

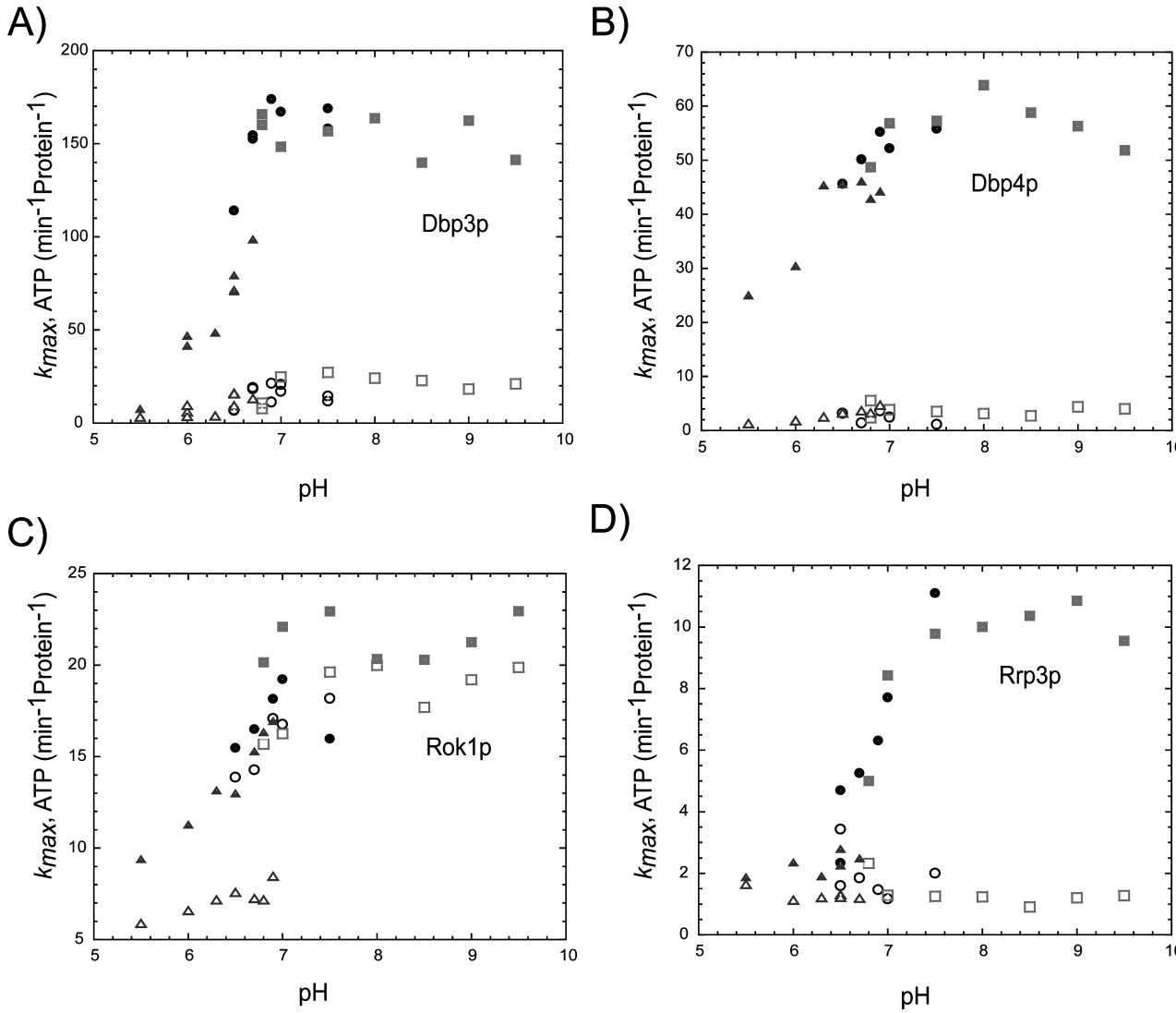

FIGURE 2: The pH dependence of ATP hydrolysis for Dbp3p (A), Dbp4p (B), Rok1p (C), and Rrp3p (D). ATP hydrolysis was measured with the NADH coupled assay with saturating (6 mM) ATP-Mg^{2+} in either 50 mM Mops (circles), Hepes (squares), or Mes (triangles) buffer. Closed symbols indicate reactions in the presence of saturating of RNA (500 nM) and open symbols in the absence of rRNA. All reactions were performed at 25 °C in 50 mM buffer, 25 mM KCl, 5 mM MgCl2, 1 mM DTT, and ATP-Mg^{2+} (6 mM).

Table 1: rRNA Steady-State Kinetic Parameters[a]

protein	$k_{obs\ No\ RNA}$ (min^{-1})	k_{cat} (min^{-1})	K_M(ATP) (mM)	k_{max} (min^{-1})	K_{app}(RNA) (nM)
Dbp3p	22 ± 4	170 ± 15	1.3 ± 0.7	183 ± 28	1.2 ± 0.6
Dbp4p	1.1 ± 0.8	50 ± 9	0.24 ± 0.09	46 ± 5	3 ± 1
Rok1p	1.4 ± 0.7	15 ± 5	1.1 ± 0.3	11 ± 2	7 ± 3
Rrp3p	0.81 ± 0.05	13 ± 4	2.3 ± 0.4	12 ± 5	5 ± 1

[a] All reactions were performed at 25 °C in 50 mM Hepes, pH 7.5 (Mes, pH 6.5 for Rok1p), 5 mM $MgCl_2$, and 1 mM DTT at saturating RNA (500 nM) or ATP (6 mM). All values represent the average of at least three independent data sets.

ics. As shown in Figure 4A and summarized in Table 1, all four proteins had k_{cat} values ranging from 13 min^{-1} to 170 min^{-1} and K_M(ATP) values ranging from 0.24 to 2.3 mM ATP. Similar values have been observed previously for several other DEAD-box proteins (*2*). The K_M(ATP) values determined for each protein were well below the concentration of cellular ATP (~5−10 mM). Presuming that the nucleolar ATP concentration is similar to the cellular concentration, these results suggest that the *in vivo* levels of ATP are saturating for all four enzymes.

The rate of ATPase activity was also measured as a function of rRNA concentration at saturating ATP to determine a k_{max} and a K_{app}(rRNA) for each protein (Figure 4B). In every case, the value of k_{max} equaled the k_{cat} obtained in the ATP titration experiments, indicating that the same E·ATP·RNA complex forms regardless of whether rRNA or ATP is saturating prior to initiation of ATP hydrolysis (Figure 4 and Table 1). Dbp3p, Dbp4p, Rok1p, and Rrp3p each showed slightly different dependencies on the rRNA concentration, with K_{app}(rRNA) values ranging from 1 to 8 nM. While these values may reflect differences in the rRNA affinities, this analysis is complicated by the fact that the number of proteins bound per rRNA may vary among the four proteins.

Because the above characterizations were performed at protein concentrations that gave easily measurable rates, and

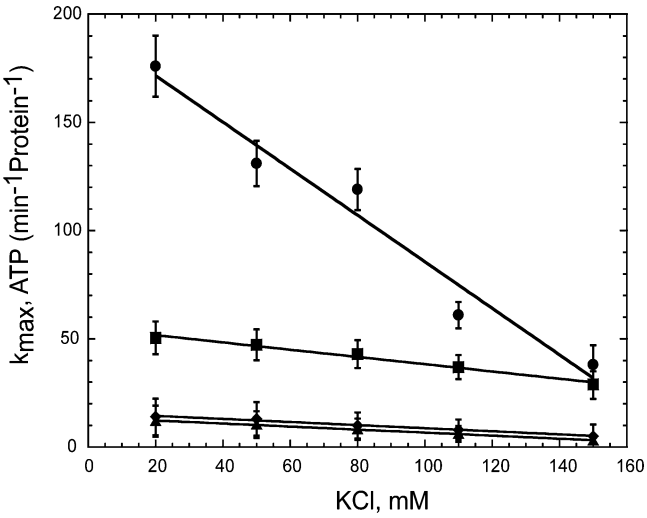

FIGURE 3: Dependence of ATP hydrolysis on KCl concentration for Dbp3p (circles), Dbp4p (squares), Rok1p (diamonds), and Rrp3p (triangles). ATP hydrolysis was measured at 25 °C in 50 mM Hepes, pH 7.5 (Mes, pH 6.5 for Rok1p), 5 mM MgCl2, 1 mM DTT, and saturating (6 mM) ATP-Mg2+ and (500 nM) RNA.

the activity of an enzyme can sometimes be influenced by its oligomeric state or multiple binding modes (*59, 60*), it was of interest to test whether the observed specific activity of Dbp3p, Dbp4p, Rok1p, and Rrp3p is affected by protein concentration. As most of the above experiments were also performed with a molar excess of rRNA over protein to populate the most favorable binding site, it was also of interest to test whether the specific activity changes when multiple proteins are present per RNA molecule. As shown in Figure 5A, the rate of ATP hydrolysis was linearly proportional to protein concentration over a range of 5 to 470 nM at 500 nM rRNA, which was in excess over the protein concentration. In Figure 5B, a similar linear proportionality was observed in the presence of 85 nM rRNA, which was saturating, but not in excess. The observation of fixed specific activity of each protein in the presence of excess RNA demonstrates that there is no evidence for the protein concentration to have either a positive or negative effect on activity. In addition, given that the specific activity is unchanged when protein is in excess of rRNA, it is evident that rRNAs contain multiple binding sites that can activate each protein to similar extents (Figure 5). Because rRNAs have many potential binding sites, it was not possible to achieve high enough protein to RNA ratios to estimate how many protein molecules a single RNA can activate.

RNA-Binding Site Size and Sequence Specificity. A set of 11 single-stranded oligonucleotides ranging from 6 to 42 residues was utilized to evaluate the length requirement of the RNA-dependent ATPase activity for each of the four proteins. A nested set of sequences with a common 5′ hexamer was designed to minimize any long stretches of self-complementary residues to avoid stable secondary structures. Since the sequences had no similarity to yeast rRNA, all 11 substrates can be considered nonspecific. The values of k_{max} and K_{app}(RNA) were obtained by titrating each oligonucleotide in the presence of saturating ATP for Dbp3p, Dbp4p, and Rrp3p (Figure 6). The overall low activity observed for Rok1p and the inability to achieve RNA saturation, even at 150 μM, prevented the determination of both k_{max} and K_{app}(RNA) for all oligomers tested. The k_{max} of Dbp3p, Dbp4p, and Rrp3p increased with increasing chain length and reached a maximal value that closely corresponded to the k_{max} obtained utilizing the rRNA substrate (Table 1). The rate of ATP hydrolysis for Rok1p, at 150 μM RNA, increased with chain length, yet only reached half of the value determined with rRNA even in the presence of the longest oligonucleotide. Interestingly, each protein required a different oligomer length for maximum activity (Figure 6A). Dbp3p was fully activated by a 10-mer RNA, Rrp3p needed at least a 16-mer, and Dbp4p required a 25-mer to obtain optimal ATP hydrolysis. For Rok1p, an extrapolation of the hydrolysis rate to the k_{max} value observed in the presence of rRNA suggests that this protein surprisingly requires at least a 90 nucleotide single-stranded RNA to achieve maximal activation. In the case of Dbp3p, Dbp4p, and Rrp3p, the lower k_{max} values observed for the shorter RNAs were not a result of RNA binding since saturation was achieved for each curve. These results indicate that the lower k_{max} values reflect the fact that the active site must not be fully organized upon binding the shorter RNAs. Thus, each protein has a characteristic single-stranded RNA site size to achieve full activity.

The values of K_{app}(RNA) for Dbp3p, Dbp4p, and Rrp3p were in agreement with the site sizes defined by the k_{max} values (Figure 6). However, the values of K_{app}(RNA) for Dbp3p and Rrp3p decreased rapidly with length until the site size was reached, reflecting additional favorable protein−RNA interactions. As the length increased further, K_{app}(RNA) decreased more slowly, presumably as a result of the thermodynamic effect of multiple binding registries (*61*). A second decrease in K_{app}(RNA) was observed for Dbp3p with a 26 oligomer where two proteins can bind the same RNA given a site size of 13 nucleotides. The K_{app}(RNA) for Dbp4p was fairly weak until a length of 22 to 26 nucleotides was reached. This dramatic increase in affinity possibly suggests the presence of strong stabilizing RNA−protein interactions near the edge of the binding site. RNA saturation was not observed even at the highest RNA concentrations tested for Rok1p, indicating that K_{app}(RNA) must be greater than 300 μM (Figure 6). Nevertheless, at the presumed fully filled site, the K_{app}(RNA) for three of the four proteins was in the low micromolar range (Dbp3p = 3 μM, Dbp4 = 0.8 μM, and Rrp3p = 5 μM). These site size binding affinities were 250- to 2500-fold weaker than the corresponding values of K_{app}(RNA) determined using rRNA as a substrate (Table 1). The disparity between the affinities for the short single-stranded RNA and rRNA substrate is consistent with the view that the long rRNA (5352 nt) contains hundreds of potential binding sites with K_{app}(RNA) values similar to those of the oligonucleotide RNAs. Hence, the binding affinity for the rRNA substrate must be normalized for length by expressing it in molar nucleotide units in order to compare the two K_{app}(RNA)s appropriately. When this is done, the binding affinity for rRNA is within 1 order of magnitude as compared to K_{app}(RNA) values for the oligonucleotides (Table 2).

The observation that rRNA contains many sites that activate ATPase activity suggests that a variety of RNA substrates could activate these proteins. This prediction was supported by the observation that in the presence of a range of structured RNA substrates, the measured k_{max} and K_{app}(RNA), in molar nucleotides, were all within 3-fold for each of the four proteins analyzed (summarized in Table 2). Both

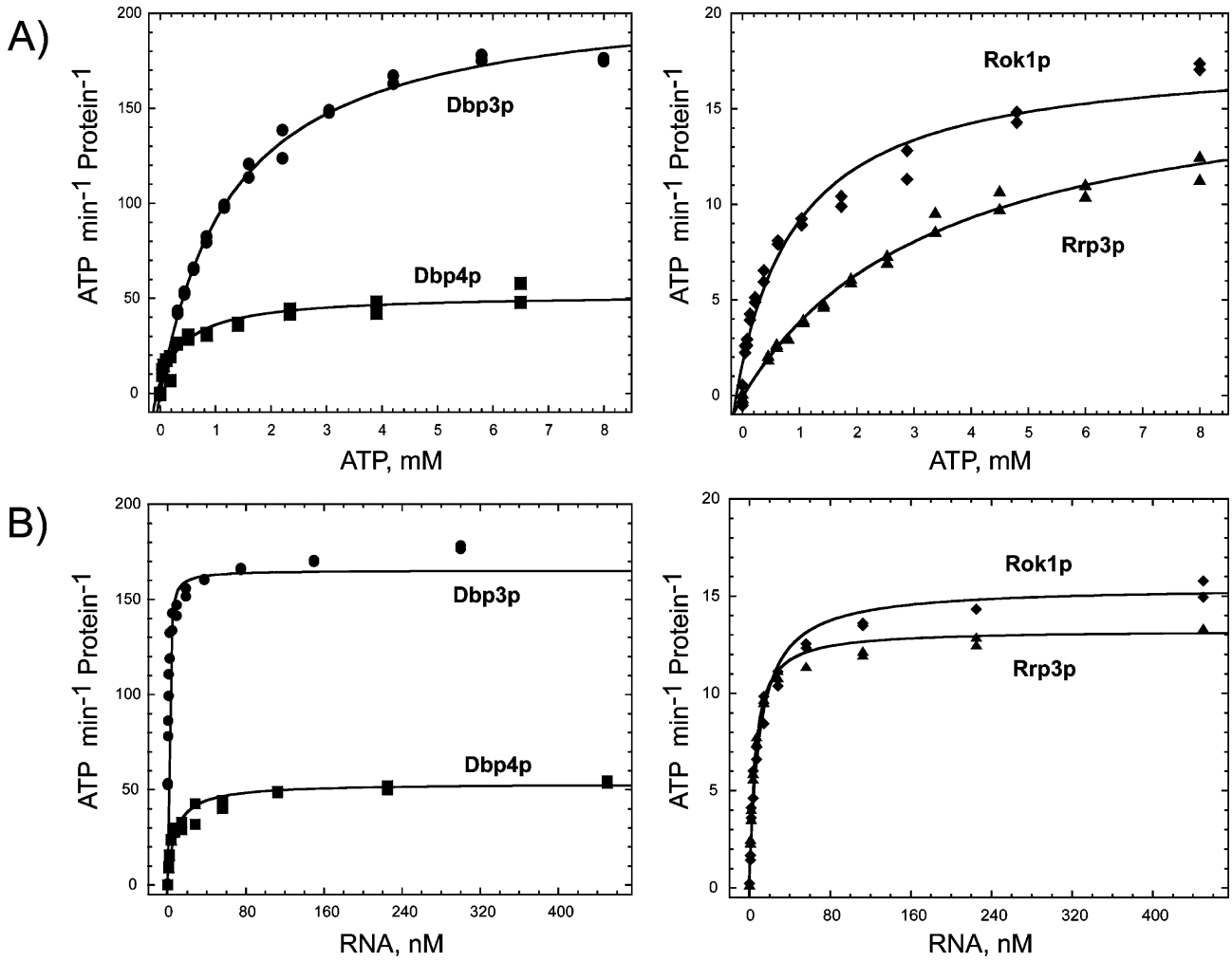

FIGURE 4: Steady-state kinetics of the ATPase activity for Dbp3p (60 nM), Dbp4p (100 nM), Rok1p (250 nM), and Rrp3p (250 nM). (A) Varying ATP concentrations in the presence of 500 nM yeast rRNA. (B) Varying rRNA concentration at 6.5 mM ATP-Mg^{2+}. The data were fit to (A) the Michaelis−Menten equation to determine k_{cat} and K_M(ATP) or (B) a complete kinetic equation (*56*) to determine k_{max} and K_{app}(RNA). Values are given in Table 1. ATP hydrolysis was measured at 25 °C in 50 mM Hepes, pH 7.5 (Mes, pH 6.5 for Rok1p), 25 mM KCl, 5 mM $MgCl_2$, and 1 mM DTT.

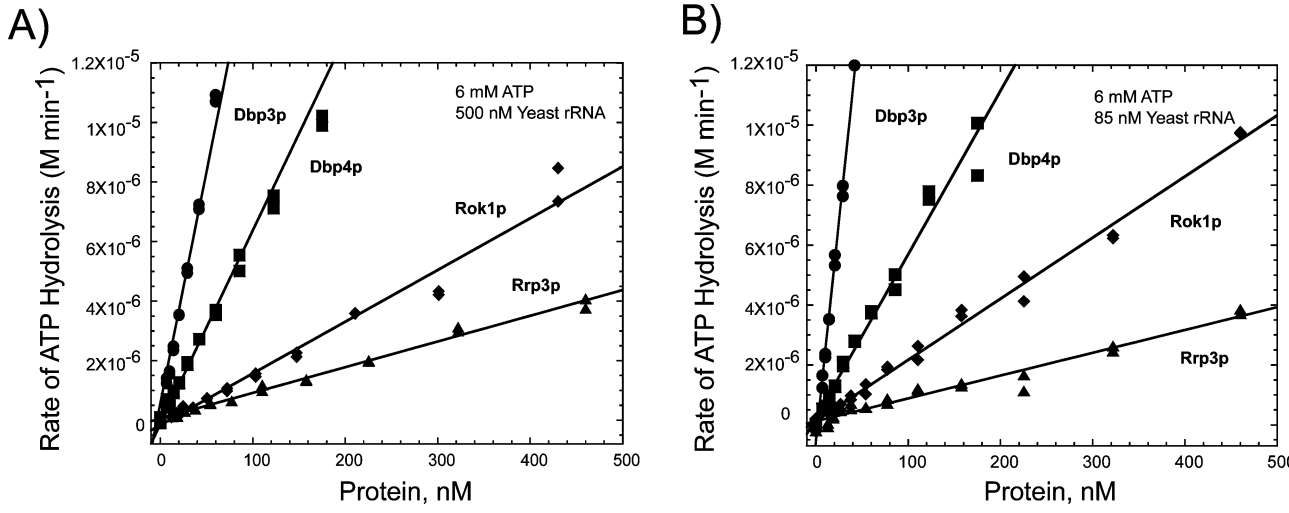

FIGURE 5: ATPase activity as a function of protein concentration at 6 mM ATP-Mg^{2+} and (A) 500 nM yeast rRNA or (B) 85 nM yeast rRNA at 25 °C in 50 mM Hepes, pH 7.5 (Mes, pH 6.5 for Rok1p), 25 mM KCl, 5 mM $MgCl_2$, and 1 mM DTT.

a random RNA transcript from the pBlue cloning vector and the group I intron RNAs stimulated the k_{max} and the K_{app}(RNA) of each protein within a factor of 3 when compared to both *E. coli* and yeast rRNAs as well as the yeast pre-rRNA (35S). The only exception was that the group I intron was a poor substrate for Rok1p. In the case of Dbp3, Dbp4p, and Rok1p, the corresponding snoRNAs, RNase MRP for Dbp3p, U14 snoRNA for Dbp4p, and snR10 snoRNA for Rok1p, also yielded k_{max} and K_{app}(RNA) values similar to those of rRNAs (Table 2). It appears that these

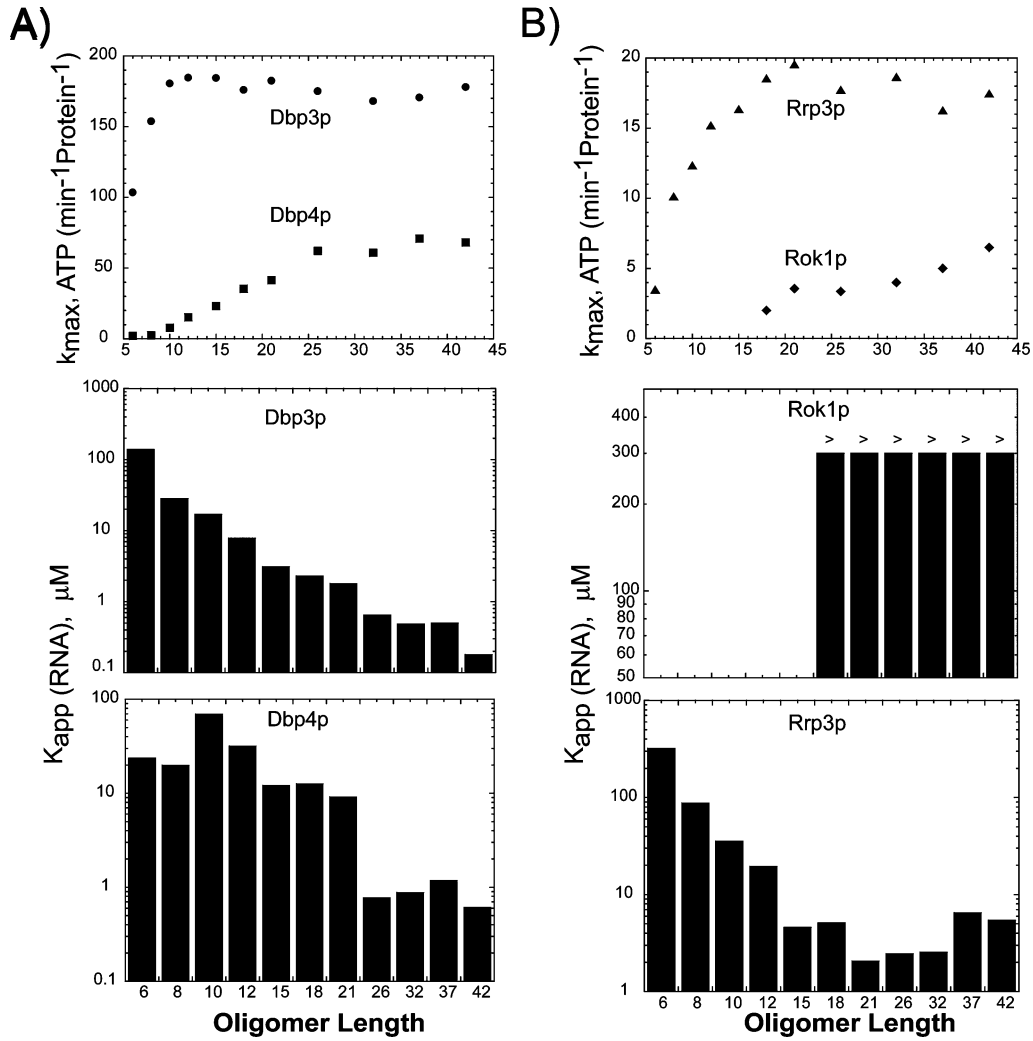

FIGURE 6: RNA site size of ATPase activity. Upper panel: k_{max} as a function of oligomer length for (A) Dbp3p (circles) and Dbp4p (squares), and (B) Rok1p (diamonds) and Rrp3p (triangles). Lower bar graphs: K_{app}(RNA) values for the same reactions. In Rok1p reactions, RNA concentrations never reached saturation, and the K_{app}(RNA) values represent a lower binding limit. ATP hydrolysis was measured at 25 °C in 50 mM Hepes, pH 7.5 (Mes, pH 6.5 for Rok1p), 25 mM KCl, 5 mM $MgCl_2$, 1 mM DTT, and saturating (6 mM) ATP-Mg^{2+}.

structured RNAs all contain many binding sites that are capable of activating each protein. Therefore, these results cannot distinguish between a lack of target specificity and specificity masked by hundreds of nonspecific sites.

The presence of a large number of nonspecific ATPase activation sites in rRNA greatly complicates the identification of a single specific site with somewhat tighter K_{app}(RNA) or faster k_{max} values that reflect the physiological binding site of each protein. For example, even if a specific site is bound 10-fold tighter, the presence of hundreds of nonspecific binding sites would result in the protein being distributed across many sites even when present in equimolar concentration with the rRNA. One approach to identifying potentially rare specific sites is to alter the buffer conditions such that nonspecific sites are suppressed without disrupting binding at the specific site. The specificity of a basic RNA binding protein can often be masked at low ionic strength due to increased affinity for all RNAs. To weaken nonspecific interaction, the K_{app}(RNA) values were also measured at a higher salt concentration (110 mM KCl) and normalized to substrate length. To confirm that the ATP concentration was still saturating during the high-salt RNA titration experiment, the K_M(ATP) was measured for each protein and was not observed to increase dramatically (Dbp3p = 1.7 mM, Dbp4p = 0.39 mM, Rok1p = 1.6 mM, and Rrp3p = 2.8 mM). An increase in the ionic strength, from 25 mM to 110 mM KCl, in the reaction showed a 2- to 6-fold increase in K_{app}(rRNA) due to competing ionic interactions. However, Dbp3, Dbp4, and Rrp3 showed negligible (2- to 5-fold) selectivity changes for yeast rRNA or 35S pre-rRNA over the nonspecific structured RNA controls (data not shown). In the case of Rok1p, the selectivity in K_{app}(RNA) for the fully matured yeast rRNA increased 12-fold compared to the nonspecific RNA controls and suggests that this protein may bind to rRNA and not the spacers of the pre-rRNA intermediates. This ionic strength analysis was complicated by the fact that all four proteins showed a moderate to substantial decrease in k_{max} as the ionic strength increased. The k_{max} and K_{app}(RNA) values for each protein would be undeterminable at the ionic strengths required to dramatically decrease nonspecific binding because of very low ATPase activity.

An indication of potential intrinsic specificity for a unique rRNA site comes from the measured ATPase activity in the presence of homopolymers, which contain equivalent binding sites (Table 2). Specifically, Dbp3, Dbp4, and Rrp3p can only be activated by RNA substrate since DNA homopolymers demonstrated nearly immeasurable activities (Table 2). In contrast, ssDNA did show some ATPase stimulation in

Table 2: Steady-State Kinetic Parameters[a]

	Dbp3p		Dbp4p		Rok1p		Rrp3p	
RNA	k_{max} (min^{-1})	K_{app} (nucleotide (μM))	k_{max} (min^{-1})	K_{app} (nucleotide (μM))	k_{max} (min^{-1})	K_{app} (nucleotide (μM))	k_{max} (min^{-1})	K_{app} (nucleotide (μM))
35S pre-rRNA	141 ± 34	6.4 ± 0.3	45 ± 2	13 ± 10	11 ± 3	108 ± 90	12 ± 1	38 ± 17
S. c. rRNA	183 ± 28	5.3 ± 0.5	46 ± 5	11 ± 7	11 ± 2	32 ± 12	12 ± 5	21 ± 9
E. c. rRNA	109 ± 25	13 ± 5	40 ± 8	18 ± 6	11 ± 1	58 ± 18	10 ± 3	40 ± 10
Rnase MRP	182 ± 19	11 ± 8						
U14 snoRNA			69 ± 10	18 ± 9				
snR10 snoRNA					16 ± 5	136 ± 100		
PTL-21	132 ± 34	12 ± 9	35 ± 5	39 ± 12	2 ± 2*	>1500	8 ± 2	97 ± 30
blue RNA	172 ± 31	11 ± 2	47 ± 7	22 ± 10	5 ± 3	30 ± 9	10 ± 4	40 ± 12
oligonucleotide	181 ± 28[b]	3.1 ± 0.9[b]	62 ± 5[c]	0.8 ± 0.3[c]	16 ± 4[d]	5 ± 3[d]		
poly A	224 ± 16	22 ± 10	24 ± 9	200 ± 100	4 ± 3	50 ± 16	14 ± 6	225 ± 100
poly U	290 ± 55	0.51 ± 0.06	11 ± 8	75 ± 20	12 ± 5	225 ± 120	15 ± 5	50 ± 12
poly C	195 ± 25	1.5 ± 0.9	49 ± 9	30 ± 17	5 ± 2	200 ± 90	7 ± 2	250 ± 120
poly I:C	73 ± 9	22 ± 11	11 ± 3	20 ± 11	3 ± 1	960 ± 400	1 ± 4	48 ± 8
poly dA	5.1 ± 0.2*	–	2 ± 3*	–	8 ± 2	110 ± 75	0.02 ± 0.02*	–
poly dA:dT	0.01 ± 0.02	–	2 ± 5*	–	1 ± 3*	–	0.2 ± 0.2*	–
salmon DNA	8 ± 2*	–	7 ± 4*	–	11 ± 5	125 ± 32	0.01 ± 0.02*	–

[a] All reactions were performed at 25°C in 50 mM Hepes, pH 7.5 (Mes, pH 6.5 for Rok1p), 5 mM $MgCl_2$, and 1 mM DTT at saturating ATP (6 mM). * Denotes reactions that could not achieve saturation. [b] Site size of 13 nt not normalized to length: units, μM. [c] Site size of 25 nt not normalized to length: units, μM. [d] Site size of 16 nt not normalized to length: units, μM. Dashes denote values that cannot be determined accurately. All values represent the average of at least three independent data sets.

the case of Rok1p. It is currently not known if this observed stimulation by DNA is biologically relevant. As shown in Table 2, the single-stranded RNA homopolymers poly (A), poly (U), and poly (C), as well as the double-stranded poly (I:C), show a much broader range of k_{max} and K_{app}(RNA) values than the mixed sequence RNAs. Interestingly, poly (U) RNA activates Dbp3p to a greater extent and binds with a 40-fold tighter affinity than poly (A). This observed preference is even more pronounced at 110 mM KCl (120-fold, data not shown). For Dbp4, Rok1p, and Rrp3p, all homopolymers bind with similar affinities except in the case of Dbp4 where the affinity for poly (A) is very weak. Nevertheless, the measured k_{max} values vary within this set of RNAs. In the case of Rrp3p, poly (A) and poly (U) stimulated ATP hydrolysis to a greater extent; whereas, poly (U) or poly (C) RNAs stimulated the ATPase activity to a greater extent with Rok1p and Dbp4p, respectively. The double-stranded RNA homopolymer did not activate hydrolysis as well as its ssRNA counterparts. However, the differences observed for Dbp4p and Rokp1 no longer held true at 110 mM KCl. In the case of Rrp3p, a modest 10-fold increase in affinity was observed for poly (U) RNA at higher ionic strength. Since k_{max} reflected the ATPase rate at saturating ATP and RNA, these discovered differences were not an indication of ATP or RNA binding but of differential architectural contacts within the ATP-binding pocket.

DISCUSSION

The four DEAD-box proteins analyzed in this study have similar conserved motifs and RecA-like core domains, and they possess general properties that are shared by all DEAD-box proteins. However, the values of k_{cat} and K_M(ATP) for each vary by approximately 10-fold in the presence of yeast rRNA. Specifically, Dbp3p is a robust ATPase with moderately weak ATP binding. Dbp4p hydrolyzes ATP slower, yet binds to ATP tighter. Rok1p and Rrp3p have weak ATPase activity and moderately weak binding affinities for ATP. The ATPase activities observed for these four DEAD-box proteins lie within the range observed for other members of this helicase subfamily. Among the subset of previously characterized DEAD-box proteins, the measured K_M(ATP) values have been reported to range from 0.065 mM to 2.3 mM (30-fold), whereas the k_{cat} values vary from 6 min^{-1} to 600 min^{-1} (100-fold) (*2*). This large range of activity is interesting especially since the signature conserved motifs form a structurally conserved binding pocket. It is quite possible that the observed variabilities in catalytic properties are partially a consequence of the RNA substrate utilized. As seen with the bacterial DEAD-box protein DbpA, the most favorable ATP binding and hydrolysis activity are only observed with the 23s rRNA substrate (*48*). Similarly, the rate of hydrolysis for Dbp3p is optimal in the presence of poly (U). Another possible explanation for the difference in activity among DEAD-box proteins is that the k_{cat} and K_M(ATP) can be affected by accessory proteins. For example, the yeast ribosome processing factor Esf2 has been shown to interact with the DEAD-box Dbp8p and subsequently increases the k_{cat} and lowers the K_M(ATP) (*57*). Additionally, the ATP binding and hydrolysis of the wheat germ DEAD-box eIF4A are also positively affected by specific protein cofactors (*62*). Alternatively, these observed differences in ATPase activity among DEAD-box proteins may reflect their distinct functions within the cell. For example, a DEAD-box protein that must undergo multiple rounds of catalysis to disrupt a complex RNA structure may be highly active compared with a protein that uses its catalytic activity solely to bind and release its substrate.

The range of ATPase activities among DEAD-box proteins is also possibly related to the structure and dynamics of the 15 highly conserved amino acids that make up the ATPase active site (*8*). Since the active site lies between the interface of two RecA-like domains, the position of the domains could possibly affect ATPase activity once an RNA is bound. In addition, nonconserved amino acids could participate in modulating hydrolysis activity since these amino acids are unique to individual DEAD-box proteins. In an attempt to correlate the variable activities with additional sequence elements in DEAD-box proteins, the 350 amino acid helicase

core sequences of all yeast DEAD-box proteins were aligned with the multiple sequence alignment program ClustalW (*63*). The alignment was utilized to create a similarity-tree with the program Phylodraw (*64*) in which 25 yeast DEAD-box proteins were observed to form groups consisting of 1 to 4 related sequences. All yeast DEAD-box proteins showed 25% sequence identity (about 80 amino acids out of 350), which corresponds to the signature DEAD-box protein conserved motifs. Surprisingly, several groups scored a 42% sequence identity (147 of 350 amino acids), which indicates additional sequence conservation outside the conserved motifs. For example, the Dbp3p helicase is closely related to DEAD-box proteins Dbp1 and Ded1, which are both involved in translation initiation, and Dbp2, which participates in mRNA degradation. Interestingly, Dbp3p and Ded1 both have robust ATP turnover rates, ranging from 150 to 300 min^{-1} (*65, 66*), suggesting that this particular group of DEAD-box proteins require rapid hydrolysis *in vivo*. The Rrp3p sequence is very similar to Dbp8p and Drs1, which both participate in rRNA processing. Of this group, Dbp8p (17 min^{-1}) and Rrp3p (13 min^{-1}) have similar ATP turnover rates (*57*). Similar alignments with Dbp4p and Rok1p were less informative. Rok1p has a core sequence that is very different from this yeast subfamily, whereas the Dbp4p core is similar to only Has1 (rRNA processing), which has a 10-fold slower rate of hydrolysis than Dbp4p (*26*). Even though this comparison is incomplete, it nonetheless suggests that certain amino acid residues located peripheral to the nine conserved DEAD-box motifs may define ATPase activities important for different functions in the cell.

A striking difference among Dbp3p, Dbp4p, Rok1p, and Rrp3p was the length of single-stranded oligonucleotide needed to obtain the same maximal rate of ATP hydrolysis observed with the rRNA substrate. In the case of Dbp3p (13 nt) and Rrp3p (16 nt), the determined site is comparable to those observed for other RNA and DNA helicases, including Rho (13 nt) (*67*), eIF-4A (13 nt) (*68, 69*), and RhlE (16 nt) (*70*). As seen in the cocrystal structures of HCV-NS3 (*7*), Rep (*71*), PcrA (*72*), and Vasa (*8*) with oligonucleotides, the site size range (8−10 nt) is consistent with the physical length needed for an oligomeric substrate to span the RecA domains and subsequently stabilize the ATP active site. Interestingly, the much larger site size observed for Dbp4p (25 nt) and Rok1p (~90 nt) suggests a more complex RNA−protein interaction in which the N- or C-terminal domains may additionally be involved in activity. Alternatively, the oligonucleotides tested may not be suitable model substrates for these two proteins. The binding of Dbp4p and Rok1p may have a modest specificity for sequences not present in the shorter oligonucleotides or may require double-helical RNA, which was minimized in the selected substrates. Nevertheless, a large site size has been observed in other RNA and DNA helicases, including CsdA (26 nt) (*70*), SrmB (36 nt) (*70*), PriA (20 nt) (*73*), and DnaB (20 nt) (*74*).

Dbp3p, Dbp4p, Rok1p, and Rrp3p showed little to no specificity *in vitro* for either the mature yeast rRNA, the 35S pre-rRNA transcript, or the corresponding snoRNAs versus the nonspecific structured control RNAs. The specificity, if present, is likely occluded by the ability of the proteins to be activated by multiple sites. These binding sites can simulate similar catalytic properties in the proteins compared to the nonspecific short oligonucleotide substrates. A relative lack of specificity has been observed with virtually all DEAD-box proteins assayed as purified proteins *in vitro*, including SrmB (*70*), RhlE (*70*), CsdA (*70*), Has1p (*26*), eIF-4A (*75*), and Dbp9p (*49*). Currently, only two proteins demonstrate substrate specificity. Prp5 shows modest specificity (10-fold) for the U2 snRNA, consistent with its function as an essential factor in the first ATP-dependent step of splicing (*50*). Similarly, the bacterial DEAD-box protein DbpA shows high specificity (>500-fold) for the 23S rRNA, consistent with its proposed role in ribosome assembly (*48*). In contrast, other DEAD-box proteins such as CYT-19 and Mss116p appear to act on multiple substrates *in vivo* and thus show little or no specificity *in vitro* (*76, 77*). One or more of the proteins studied in this work may have an intrinsic specificity for a region within the rRNA. However, this specificity may be obscured by the presence of multiple nonspecific sites, which may be an artifact of the very basic nature of the proteins. Attempts to reveal such specific sites by varying the RNA to protein ratio and by altering the ionic strength were unsuccessful. Unfortunately, determination of specific RNA targets for the NTE or CTE is difficult because *in vitro* reconstruction of actual RNA structural intermediates of the rRNA processing pathway is not yet possible. Nevertheless, experiments with homopolymers revealed an interestingly strong (35-fold) specificity of Dbp3p for poly (U). Previous studies have shown that Dbp3p can stimulate the cleavage of site A3 within the ITS1 spacer during rRNA processing (*33*). According to the secondary structure model, ITS1 contains two U-rich single-stranded regions between cleavage sites A2 and A3, and one larger region downstream of A3 (Figure 1A). Consequently, Dbp3p's preference for poly (U) sequences may be indicative of Dbp3p binding and acting at one or more of the three U-rich single-stranded regions in the ITS1 spacer proximal to the A3 cleavage site. The observed poly (U) targeting for Dbp3p is consistent with other *trans*-acting factors that affect ITS1 processing such as Rrp5, which also has a specificity for poly (U) substrates (*78*−*80*). Preliminary attempts to demonstrate Dbp3p specificity for rRNA subfragments were unsuccessful and resulted in uniform ATPase activities. Additionally, direct binding studies have shown that the Dbp3p binds these subfragments uniformly.

The lack of specificity for a particular RNA site *in vitro* contradicts the ability of Dbp3p, Dbp4p, Rok1p, and Rrp3p to act specifically at certain stages of the ribosome assembly pathway. As predicted from *in vivo* studies, the selected enzymes normally function on complex RNP substrates and probably need other protein cofactors and/or a specific RNA conformation that is not present in free rRNA. While Dbp3, Dbp4, Rok1p, and Rrp3 may be recruited spatially and temporally by specific interactions with an RNP, it cannot be ruled out that they could act catalytically on multiple nearby regions of the pre-rRNA during assembly. This possibility could also explain the proteins' ability to achieve activation by such a variety of RNA sequences.

ACKNOWLEDGMENT

We thank Dr. Margaret E. Saks, Dr. Fedor Karginov, Dr. Lisa Ellis-Sharpe, Dr. Kevin Polach, Sarah Ledoux, and Kevin Keegan for many stimulating discussions and a careful reading of the manuscript. The *S. cerevisiae* Lhy1 strain was

generously supplied by Dr. Linda Hicke, and the *S. cerevisiae* EJ101 strain was generously supplied by Dr. Erik J. Sontheimer.

REFERENCES

1. Rocak, S., and Linder, P. (2004) DEAD-box proteins: the driving forces behind RNA metabolism. *Nat. Rev. Mol. Cell Biol. 5* (3), 232–41.
2. Cordin, O., Banroques, J., Tanner, N. K., and Linder, P. (2006) The DEAD-box protein family of RNA helicases. *Gene 367*, 17–37.
3. Gorbalenya, A. E., and Koonin, E. V. (1993) Helicases: amino acid sequence comparisons and structure-function relationships. *Curr. Opin. Struct. Biol. 3*, 419–429.
4. Tanner, N. K., Cordin, O., Banroques, J., Doere, M., and Linder, P. (2003) The Q motif: a newly identified motif in DEAD box helicases may regulate ATP binding and hydrolysis. *Mol. Cell 11* (1), 127–38.
5. Story, R. M., and Steitz, T. A. (1992) Structure of the recA protein−ADP complex. *Nature 355*, 374–376.
6. Caruthers, J. M., and McKay, D. B. (2002) Helicase structure and mechanism. *Curr. Opin. Struct. Biol. 12*, 123–133.
7. Kim, J. L., Morgenstern, K. A., Griffith, J. P., Dwyer, M. D., Thomson, J. A., Murcko, M. A., Lin, C., and Caron, P. R. (1998) Hepatitis C virus NS3 RNA helicase domain with a bound oligonucleotide: The crystal structure provides insights into the mode of unwinding. *Structure 6*, 89–100.
8. Sengoku, T., Nureki, O., Nakamura, A., Kobayashi, S., and Yokoyama, S. (2006) Structural basis for RNA unwinding by the DEAD-box protein Drosophila Vasa. *Cell 125* (2), 287–300.
9. Karginov, F. V., Caruthers, J. M., Hu, Y., McKay, D. B., and Uhlenbeck, O. C. (2005) YxiN is a modular protein combining a DEx(D/H) core and a specific RNA-binding domain. *J. Biol. Chem. 280* (42), 35499–505.
10. Kossen, K., Karginov, F. V., and Uhlenbeck, O. C. (2002) The carboxy-terminal domain of the DExDH protein YxiN is sufficient to confer specificity for 23S rRNA. *J. Mol. Biol. 324* (4), 625–36.
11. Silverman, E., Edwalds-Gilbert, G., and Lin, R. J. (2003) DExD/H-box proteins and their partners: Helping RNA helicases unwind. *Gene 312*, 1–16.
12. Schwer, B. (2001) A new twist on RNA helicases: DExH/D box proteins as RNPases. *Nat. Struct. Biol. 8* (2), 113–6.
13. Jankowsky, E., Gross, C. H., Shuman, S., and Pyle, A. M. (2001) Active disruption of an RNA-protein interaction by a DExH/D RNA helicase. *Science 291* (5501), 121–5.
14. Diges, C. M., and Uhlenbeck, O. C. (2001) *Escherichia coli* DbpA is an RNA helicase that requires hairpin 92 of 23S rRNA. *EMBO J. 20*, 5503–12.
15. Jankowsky, E., Gross, C. H., Shuman, S., and Pyle, A. M. (2000) The DExH protein NPH-II is a processive and directional motor for unwinding RNA. *Nature 403*, 447–51.
16. Levin, M. K., and Patel, S. S. (2003) Helicases as Molecular Motors, in *Molecular Motor* (Schliwa, M., Ed.) pp 179−206, Wiley-VCH Verlag GmbH & Co. KGaA, Weinheim, Germany.
17. Soultanas, P., and Wigley, D. B. (2001) Unwinding the 'Gordian knot' of helicase action. *Trends Biochem. Sci. 26* (1), 47–54.
18. Bjornson, K. P., Amaratunga, M., Moore, K. J., and Lohman, T. M. (1994) Single-turnover kinetics of helicase-catalyzed DNA unwinding monitored continuously by fluorescence energy transfer. *Biochemistry 33* (47), 14306–14316.
19. Elles, L. M., and Uhlenbeck, O. C. (2008) Mutation of the arginine finger in the active site of *Escherichia coli* DbpA abolishes ATPase and helicase activity and confers a dominant slow growth phenotype. *Nucleic Acids Res. 36* (1), 41–50.
20. Bernstein, K. A., Granneman, S., Lee, A. V., Manickam, S., and Baserga, S. J. (2006) Comprehensive mutational analysis of yeast DEXD/H box RNA helicases involved in large ribosomal subunit biogenesis. *Mol. Cell. Biol. 26* (4), 1195–208.
21. Granneman, S., Bernstein, K. A., Bleichert, F., and Baserga, S. J. (2006) Comprehensive mutational analysis of yeast DEXD/H box RNA helicases required for small ribosomal subunit synthesis. *Mol. Cell. Biol. 26* (4), 1183–94.
22. Daugeron, M. C., and Linder, P. (2001) Characterization and mutational analysis of yeast Dbp8p, a putative RNA helicase involved in ribosome biogenesis. *Nucleic Acids Res. 29* (5), 1144–55.
23. Turner, A. M., Love, C. F., Alexander, R. W., and Jones, P. G. (2007) Mutational analysis of the *Escherichia coli* DEAD box protein CsdA. *J. Bacteriol. 189* (7), 2769–76.
24. Shibuya, T., Tange, T. O., Stroupe, M. E., and Moore, M. J. (2006) Mutational analysis of human eIF4AIII identifies regions necessary for exon junction complex formation and nonsense-mediated mRNA decay. *RNA 12* (3), 360–74.
25. Martin, A., Schneider, S., and Schwer, B. (2002) Prp43 is an essential RNA-dependent ATPase required for release of lariat-intron from the spliceosome. *J. Biol. Chem. 277* (20), 17743–50.
26. Rocak, S., Emery, B., Tanner, N. K., and Linder, P. (2005) Characterization of the ATPase and unwinding activities of the yeast DEAD-box protein Has1p and the analysis of the roles of the conserved motifs. *Nucleic Acids Res. 33* (3), 999–1009.
27. Oh, J., and Kim, J. (1999) ATP hydrolysis activity of the DEAD box protein Rok1p is required for in vivo ROK1 function. *Nucleic Acids Res. 27*, 2753–2759.
28. Kressler, D., Linder, P., and de la Cruz, J. (1999) Protein trans-acting factors involved in ribosome biogenesis. *Mol. Cell. Biol. 19*, 7897–7912.
29. Warner, J. R., Vilardell, J., and Sohn, J. H. (2001) Economics of Ribosome Biosynthesis, in *The Ribosome: Proceedings of 2001 Symposium LXVI* (Stillman, B., Ed.) pp 567−74, Cold Spring Harbor Laboratory Press, Cold Spring Harbor, NY.
30. Venema, J., and Tollervey, D. (1999) Ribosome synthesis in *Saccharomyces cerevisiae*. *Annu. Rev. Genet. 33*, 261–311.
31. de la Cruz, J., Kressler, D., and Linder, P. (1999) Unwinding RNA in *Saccharomyces cerevisiae*: DEAD-box proteins and related families. *Trends Biochem. Sci. 24*, 192–198.
32. Tschochner, H., and Hurt, E. (2003) Pre-ribosomes on the road from the nucleolus to the cytoplasm. *Trends Cell Biol 13* (5), 255–63.
33. Weaver, P. L., Sun, C., and Chang, T. (1997) Dbp3p, a putative RNA helicase in *Saccharomyces cerevisiae* is required for efficient pre-rRNA processing predominantly at site A3. *Mol. Cell. Biol. 17*, 1354–1365.
34. Morrissey, J. P., and Tollervey, D. (1995) Birth of the snoRNPs: The evolution of RNase MRP and the eukaryotic pre-rRNA-processing system. *Trends Biochem. Sci. 20* (2), 78–82.
35. Chu, S., Archer, R. H., Zengel, J. M., and Lindahl, L. (1994) The RNA of RNase MRP is required for normal processing of ribosomal RNA. *Proc. Natl. Acad. Sci. U.S.A. 91* (2), 659–63.
36. Lygerou, Z., Allmang, C., Tollervey, D, and Seraphin, B. (1996) Accurate processing of a eukaryotic precursor ribosomal RNA by ribonuclease MRP in vitro. *Science 272* (5259), 268–70.
37. Chang, D. D., and Clayton, D. A. (1987) A mammalian mitochondrial RNA processing activity contains nucleus-encoded RNA. *Science 235* (4793), 1178–84.
38. Liang, W. Q., Clark, J. A., and Fournier, M. J. (1997) The rRNA-processing function of the yeast U14 small nucleolar RNA can be rescued by a conserved RNA helicase-like protein. *Mol. Cell. Biol. 17*, 4124–4132.
39. Dunbar, D. A., and Baserga, S. J. (1998) The U14 snoRNA is required for 2′-O-methylation of the pre-18S rRNA in Xenopus oocytes. *RNA 4* (2), 195–204.
40. Liang, W. Q., and Fournier, M. J. (1995) U14 base-pairs with 18S rRNA: a novel snoRNA interaction required for rRNA processing. *Genes Dev. 9* (19), 2433–43.
41. Morrissey, J. P., and Tollervey, D. (1997) U14 small nucleolar RNA makes multiple contacts with the pre-ribosomal RNA. *Chromosoma 105* (7−8), 515–22.
42. Kos, M., and Tollervey, D. (2005) The Putative RNA Helicase Dbp4p Is Required for Release of the U14 snoRNA from Preribosomes in *Saccharomyces cerevisiae*. *Mol. Cell 20* (1), 53–64.
43. Venema, J., Bousquet-Antonelli, C., Gelugne, J. P., Caizergues-Ferrer, M., and Tollervey, D. (1997) Rok1p is a putative RNA helicase required for rRNA processing. *Mol. Cell. Biol. 17* (6), 3398–407.
44. Ni, J., Tien, A. L., and Fournier, M. J. (1997) Small nucleolar RNAs direct site-specific synthesis of pseudouridine in ribosomal RNA. *Cell 89* (4), 565–73.
45. Samarsky, D. A., and Fournier, M. J. (1999) A comprehensive database for the small nucleolar RNAs from *Saccharomyces cerevisiae*. *Nucleic Acids Res. 27* (1), 161–4.
46. Tollervey, D. (1987) A yeast small nuclear RNA is required for normal processing of pre-ribosomal RNA. *EMBO J. 6* (13), 4169–75.

47. O'Day, C., Chavanikamannil, F., and Abelson, J. (1996) 18S rRNA processing requires the RNA helicase-like protein Rrp3. *Nucleic Acids Res. 24*, 3201–3207.
48. Tsu, C. A., and Uhlenbeck, O. C. (1998) Kinetic analysis of the RNA-dependent adenosine triphosphatase activity of DbpA, an *Escherichia coli* DEAD protein specific for 23S ribosomal RNA. *Biochemistry 37*, 16989–16996.
49. Kikuma, T., Ohtsu, M., Utsugi, T., Koga, S., Okuhara, K., Eki, T., Fujimori, F., and Murakami, Y. (2004) Dbp9p, a member of the DEAD box protein family, exhibits DNA helicase activity. *J. Biol. Chem. 279* (20), 20692–8.
50. O'Day, C. L., Dalbadie-McFarland, G., and Abelson, J. (1996) The *Saccharomyces cerevisiae* Prp5 protein has RNA-dependent ATPase activity with specificity for U2 small nuclear RNA. *J. Biol. Chem. 271* (52), 33261–7.
51. Selby, C. P., and Sancar, A. (1993) Molecular mechanism of transcription-repair coupling. *Science 260* (5104), 53–8.
52. Richmond, E., and Peterson, C. L. (1996) Functional analysis of the DNA-stimulated ATPase domain of yeast SWI2/SNF2. *Nucleic Acids Res. 24* (19), 3685–92.
53. Hall, M. C., and Matson, S. W. (1999) Helicase motifs: the engine that powers DNA unwinding. *Mol. Microbiol. 34*, 867–877.
54. Dunn, R., and Hicke, L. (2001) Multiple roles for Rsp5p-dependent ubiquitination at the internalization step of endocytosis. *J. Biol. Chem. 276* (28), 25974–81.
55. Thweatt, R., and Lee, J. C. (1990) Yeast precursor ribosomal RNA. Molecular cloning and probing the higher-order structure of the internal transcribed spacer I by kethoxal and dimethylsulfate modification. *J. Mol. Biol. 211* (2), 305–20.
56. Kossen, K., and Uhlenbeck, O. C. (1999) Cloning and biochemical characterization of *Bacillus subtilis* YxiN, a DEAD protein specifically activated by 23S rRNA: delineation of a novel subfamily of bacterial DEAD proteins. *Nucleic Acids Res. 27*, 3811–3820.
57. Granneman, S., Lin, C., Champion, E. A., Nandineni, M. R., Zorca, C., and Baserga, S. J. (2006) The nucleolar protein Esf2 interacts directly with the DExD/H box RNA helicase, Dbp8, to stimulate ATP hydrolysis. *Nucleic Acids Res. 34* (10), 3189–99.
58. Franca, R., Belfiore, A., Spadari, S., and Maga, G. (2007) Human DEAD-box ATPase DDX3 shows a relaxed nucleoside substrate specificity. *Proteins 67* (4), 1128–37.
59. Wong, I., and Lohman, T. M. (1992) Allosteric effects of nucleotide cofactors on *Escherichia coli* Rep helicase-DNA binding. *Science 256* (5055), 350–5.
60. Garcia, I, and Weeks, K. M. (2004) Structural basis for the self-chaperoning function of an RNA collapsed state. *Biochemistry 43* (48), 15179–86.
61. McGhee, J. D., and von Hippel, P. H. (1974) Theoretical aspects of DNA-protein interactions: Co-operative and non-co-operative binding of large ligands to a one-dimensional homogeneous lattice. *J. Mol. Biol. 86* (2), 469–89.
62. Bi, X., and Goss, D. J. (2000) Wheat germ poly(A)-binding protein increases the ATPase and the RNA helicase activity of translation initiation factors eIF4A, eIF4B, and eIF-iso4F. *J. Biol. Chem. 275* (23), 17740–6.
63. Linder, P. (1999) RNA helicases from the baker's yeast *Saccharomyces cerevisiae*, http://medweb2.unige.ch/~linder/RNA_helicases.html (accessed July 2008).
64. Choi, J. H., Jung, H. Y., Kim, H. S., and Cho, H. G. (2000) PhyloDraw: a phylogenetic tree drawing system. *Bioinformatics 16* (11), 1056–8.
65. Cordin, O., Tanner, N. K., Doere, M., Linder, P., and Banroquez, J. (2004) The newly discovered Q motif of DEAD-box RNA helicases regulates RNA-binding and helicase activity. *EMBO J. 23* (13), 2478–87.
66. Iost, I., Dreyfus, M., and Linder, P. (1999) Ded1p, a DEAD-box protein required for translation initiation in *Saccharomyces cerevisiae*, is an RNA helicase. *J. Biol. Chem. 274* (25), 17677–83.
67. McSwiggen, J. A., Bear, D. G., and von Hippel, P. H. (1988) Interactions of *Escherichia coli* transcription termination factor rho with RNA. I. Binding stoichiometries and free energies. *J. Mol. Biol. 199* (4), 609–22.
68. Goss, D. J., Woodley, C. L., and Wahba, A. J. (1987) A fluorescence study of the binding of eucaryotic initiation factors to messenger RNA and messenger RNA analogues. *Biochemistry 26* (6), 1551–6.
69. Abramson, R. D., Dever, T. E., Lawson, T. G., Ray, B. K., Thach, R. E., and Merrick, W. C. (1987) The ATP-dependent interaction of eukaryotic initiation factors with mRNA. *J. Biol. Chem. 262* (8), 3826–32.
70. Bizebard, T., Ferlenghi, I., Iost, I., and Dreyfus, M. (2004) Studies on three *E. coli* DEAD-box helicases point to an unwinding mechanism different from that of model DNA helicases. *Biochemistry 43* (24), 7857–66.
71. Korolev, S., Hsieh, J., Gauss, G. H., Lohman, T. M., and Waksman, G. (1997) Major domain swiveling revealed by the crystal structures of complexes of *E. coli* Rep helicase bound to single-stranded DNA and ADP. *Cell 90* (4), 635–47.
72. Velankar, S. S., Soultanas, P., Dillingham, M. S., Subramanya, H. S., and Wigley, D. B. (1999) Crystal structures of complexes of PcrA DNA helicase with a DNA substrate indicate an inchworm mechanism. *Cell 97* (1), 75–84.
73. Jezewska, M. J., Rajendran, S., and Bujalowski, W. (2000) *Escherichia coli* replicative helicase PriA protein-single-stranded DNA complex. Stoichiometries, free energy of binding, and cooperativities. *J. Biol. Chem. 275* (36), 27865–73.
74. Jezewska, M. J., Kim, U. S., and Bujalowski, W. (1996) Binding of *Escherichia coli* primary replicative helicase DnaB protein to single-stranded DNA. Long-range allosteric conformational changes within the protein hexamer. *Biochemistry 35* (7), 2129–45.
75. Rogers, G. W., Jr., Lima, W. F., and Merrick, W. C. (2001) Further characterization of the helicase activity of eIF4A. Substrate specificity. *J. Biol. Chem. 276* (16), 12598–608.
76. Mohr, S., Stryker, J. M., and Lambowitz, A. M. (2002) A DEAD-box protein functions as an ATP-dependent RNA chaperone in group I intron splicing. *Cell 109* (6), 769–79.
77. Halls, C., Mohr, S., Del Campo, M., Yang, Q., Jankowsky, E., and Lambowitz, A. M. (2007) Involvement of DEAD-box proteins in group I and group II intron splicing. Biochemical characterization of Mss116p, ATP hydrolysis-dependent and -independent mechanisms, and general RNA chaperone activity. *J. Mol. Biol. 365* (3), 835–55.
78. de Boer, P., Vos, H. R., Faber, A. W., Vos, J. C., and Raue, H. A. (2006) Rrp5p, a trans-acting factor in yeast ribosome biogenesis, is an RNA-binding protein with a pronounced preference for U-rich sequences. *RNA 12*, 263–271.
79. Torchet, C., Jacq, C., and Hermann-Le Denmat, S. (1998) Two mutant forms of the S1/TPR-containing protein Rrp5p affect the 18S rRNA synthesis in *Saccharomyces cerevisiae*. *RNA 4*, 1636–1652.
80. Venema, J., and Tollervey, D. (1996) RRP5 is required for formation of both 18S and 5.8S rRNA in yeast. *EMBO J. 15*, 5701–5714.

BI8016119